PERGAMON

Journal of Quantitative Spectroscopy & Radiative Transfer 64 (2000) 467–482

Journal of Quantitative Spectroscopy & Radiative Transfer

www.elsevier.com/locate/jqsrt

Wavenumbers, strengths, widths and shifts with pressure of lines in four bands of gaseous $^{16}O_2$ in the systems $a^1\Delta_g - X^3\Sigma_g^-$ and $b^1\Sigma_g^+ - X^3\Sigma_g^-$

Swee-Lan Cheah, Yuan-Pern Lee*[,1], J.F. Ogilvie[2]

Department of Chemistry, National Tsing Hua University, Kuang Fu Road, Hsinchu 30043, Taiwan

Abstract

In spectra of gaseous oxygen at 299 K with pressure/bar in the range [0.13,1.06] and lengths of absorbing path up to 107 m, we measured the wavenumbers, strengths, widths and shifts with pressure of 118 mostly fully resolved lines of $^{16}O_2$ due to rotational fine structure in the band $a\,^1\Delta_g(v=0) - X\,^3\Sigma_g^-(v=0)$, 59 lines in the band $b\,^1\Sigma_g^+(v=0) - X\,^3\Sigma_g^-(v=0)$, 58 lines in the band $b\,^1\Sigma_g^+(v=1) - X\,^3\Sigma_g^-(v=0)$ and 43 lines in the band $b\,^1\Sigma_g^+(v=2) - X\,^3\Sigma_g^-(v=0)$; the latter band is measured quantitatively for the first time. Spectral parameters to reproduce wavenumber data are considerably improved over previously existing data. Band strengths, average widths and shifts of lines with pressure of pure O_2 are presented, and extensive comparison of these results is made with corresponding values from the literature.

Keywords: $a\,^1\Delta_g - X\,^3\Sigma_g^-$; $b\,^1\Sigma_g^+ - X\,^3\Sigma_g^-$; O_2; Line strength; Absorption; Line width; Line shift

1. Introduction

Oxygen (O_2) is one of two diatomic molecular gaseous substances that are common in the terrestrial atmosphere, but is generally much less abundant in atmospheres of other known astronomical bodies. Besides its more or less intense electronic systems in the ultraviolet spectral

* Corresponding author. Fax: 00-886-3-5722892.

E-mail addresses: yplee@net.nthu.edu.tw (Y.-P. Lee), ogilvie@cecm.sfu.ca (J.F. Ogilvie)

[1] Jointly appointed by the Institute of Atomic and Molecular Sciences, Academia Sinica, Taipei 10764, Taiwan.

[2] Department of Chemistry, Oregon State University, Corvallis, OR 97331-4003, USA, and Department of Chemistry, University of the Witwatersrand, Private Bag 3, P.O. WITS 2050, Johannesburg, South Africa; Permanent address: Centre for Experimental and Constructive Mathematics, Simon Fraser University, Burnaby, BC V5A 1S6, Canada.

PII: S0022-4073(99)00126-0

region, oxygen has two further systems in the near infrared and visible regions that are atypically weak. With absorbing substance in a sufficiently long path and with sensitive means of detection, bands in these systems exhibit well-developed rotational fine structure that amply reveals the symmetry of electronic states between which these transitions occur [1].

These transitions are important in relation to radiative properties of the terrestrial atmosphere; at an altitude of about 70 km, up to a sixth of the heating of the gas there present, depending on latitude, results from absorption of solar energy by O_2 in red and infrared regions and subsequent exothermic chemical reactions [2]. As the basis of quantitative modeling of these effects, there are still few comprehensive measurements of strengths of spectral lines in pertinent bands, and of widths and shifts of individual lines caused by collisions either between molecules of oxygen or of these molecules with other atomic and molecular species. For the earliest precise measurements the terrestrial atmosphere served as an absorbing sample and the sun as source, with photographic plates as detectors. In most subsequent experiments either laser diodes or an interferometric spectrophotometer served as essential elements for such measurements of laboratory samples in absorption or emission.

In previous measurements in this laboratory [3] an absorbing path of maximum length 20 m was available, with which we undertook estimates of strengths of spectral lines in one band of a system in the near-infrared region, $a\,{}^1\Delta_g(v=0) - X\,{}^3\Sigma_g^-(v=0)$. Since those measurements, we acquired a new interferometric spectrophotometer equipped with two cells for gases, one having an optical path of maximum length 107 m, and with improved band filters to limit the range of wavenumber of radiation reaching a detector. We also obtained new software that is supposed to enable increasingly precise fitting of spectral lines. Hence we repeated the measurement of the former band because of its importance in relation to monitoring the concentration of atmospheric ozone [2], and included three others in the system $b\,{}^1\Sigma_g^+(v=0,1,2) - X\,{}^3\Sigma_g^-(v=0)$ in the red region of the visible spectrum. Although our measurements were all made at 299 ± 1 K we varied the pressure/bar of pure oxygen in a range [0.13, 1.06]. These experiments enable estimation of not only wavenumbers and strengths of individual lines but also shifts and widths as a function of density of a sample. Results of these measurements and their comparison with literature values are the subject of this report. In accordance with recommendations of IUPAC and IUPAP we employ SI units throughout this article [4].

2. Experiments

All spectra were recorded with an evacuated Fourier-transform interferometric spectrophotometer (Bomem DA8) and one or other cell containing gaseous oxygen (nominal purity 99.97%, used without further purification). Both optical cells employed multiple internal reflections, but with maximum paths of absorbing sample either 6 or 107 m. In the latter cell (Infrared Analysis, Model 100) of length 1.375 m between the mirrors, a series of spots on these mirrors from a He–Ne laser enabled a precise count of the number of passes of the beam through a particular sample, to define the total length in increments eight times the base path varied on adjusting the angle of a field mirror. For all measurements we employed a beam splitter made of fused silica; for the band near $7.9 \times 10^5\ \mathrm{m}^{-1}$ an InSb detector was cooled to 77 K, whereas for the other bands, individually measured, an avalanche Si detector at ambient temperature served. Optical filters (suppliers and pass bands in $m^{-1}/10^6$ specified parenthetically) are S906300 (ESCO Products, 1.565–1.605), S907650 (ESCO, 1.29–1.33), S906900 (ESCO, 1.43–1.47), and 1200WB200 (Omega, 0.76–0.89). Typical resolution 2.5–3.0 m^{-1} (6.0 m^{-1} for the band near 1.58×10^6 m^{-1}) was chosen so that the best ratios of signal to noise were achieved within a practicable duration of collection of interferograms, not more than 20 h; resolution is specified as the reciprocal of the maximum path difference between the split beams of the interferometer. Calibration of the wavenumber scale was made in the vicinity of each band by means of a neon discharge lamp as an emission source [5], except I_2 vapor [6] in an absorption cell for the band near 1.58×10^6 m^{-1}; differences between measured and standard wavenumbers were less than ~ 1.7 m^{-1} in all cases, and the corresponding corrections, $+1.6$ m^{-1} for the band near 7.9×10^5 and $+0.7$ m^{-1} for each of the other three bands, were accordingly applied to values of wavenumbers reported in our tables. The temperature of each gas cell was monitored with two thermocouples of type K indicating minimum and maximum temperatures during a period that interferograms were collected; the maximum variation during an acceptable scan was less than 1 K near 299 K. The pressure of gaseous sample in either cell, within a range/bar [0.13, 1.06], was measured before and after each collection of interferograms with a capacitance manometer (MKS model 221A). For some samples we also tested the effect of varied length of optical path at a constant pressure.

Spectra were analyzed with software (Grams, Galactic Industries Corporation) designed to operate with the spectrometer. Each co-added interferogram accumulated over many hours was converted via its Fourier transform into a spectrum with apparent energy as a function of wavenumber. Successive operations of collection of a reference spectrum and conversion of the ratio to transmittance and absorbance yielded spectra such as those presented in Figs. 1–4 for measured bands; these figures demonstrate a ratio of signal to noise achieved with our improved instruments and spectral processing. With each spectrum in a form absorbance versus

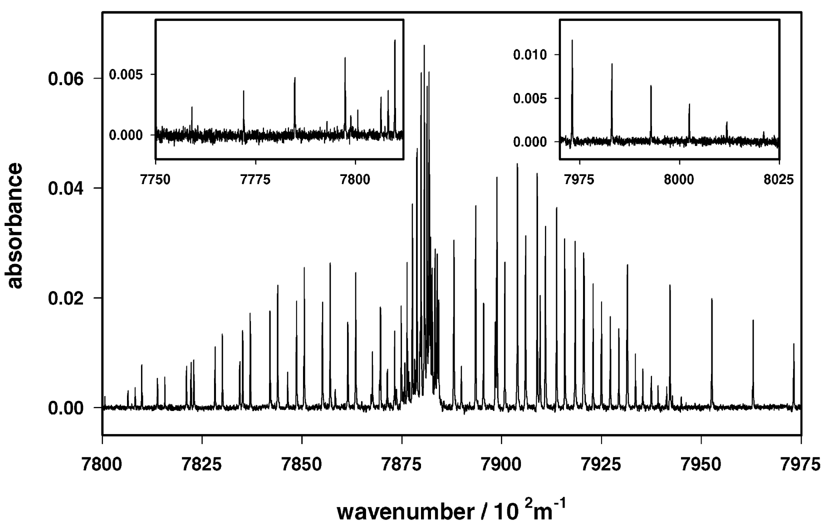

Fig. 1. Absorption spectrum of gaseous $^{16}O_2$ in the band $a\,^1\Delta_g(v=0) - X\,^3\Sigma_g^-(v=0)$; length of absorption path 85 m, pressure 1.06 bar, temperature 299 K; insets show wings of the band on an expanded scale of ordinate.

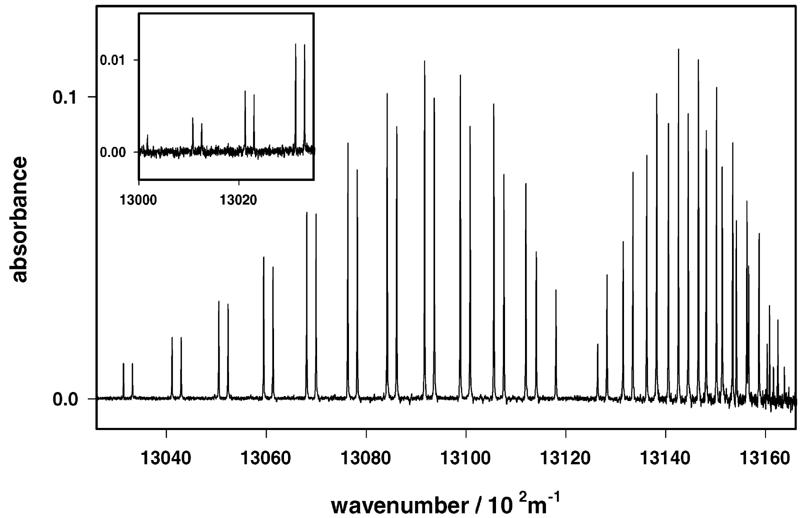

Fig. 2. Absorption spectrum of gaseous $^{16}O_2$ in the band $b\,^1\Sigma_g^+(v=0) - X\,^3\Sigma_g^-(v=0)$; length of absorption path 3 m, pressure 0.66 bar, temperature 299 K; insets show wings of the band on an expanded scale of ordinate.

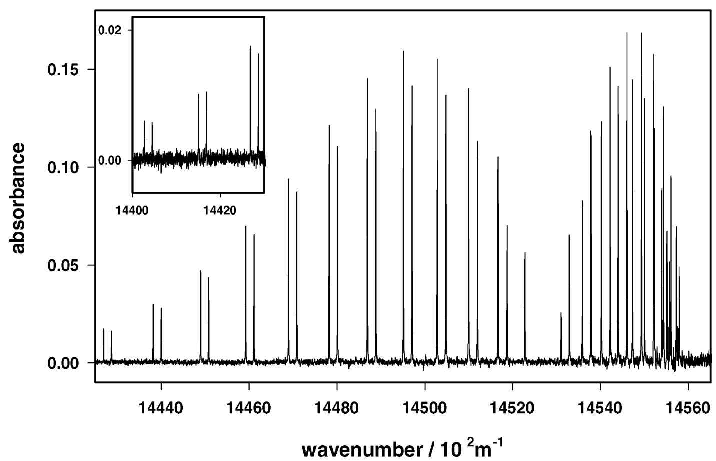

Fig. 3. Absorption spectrum of gaseous $^{16}O_2$ in the band $b\,^1\Sigma_g^+(v=1) - X\,^3\Sigma_g^-(v=0)$; length of absorption path 74 m, pressure 0.40 bar, temperature 299 K; insets show wings of the band on an expanded scale of ordinate.

wavenumber, each detectable line was fitted according to a Lorentzian shape. For samples at pressures greater than 0.38 bar, tests on intense lines with a variable combination of Gaussian and Lorentzian profile confirmed that their shapes were well described with a Lorentzian function alone, with no significant component of Gaussian form empirically required; a Gaussian

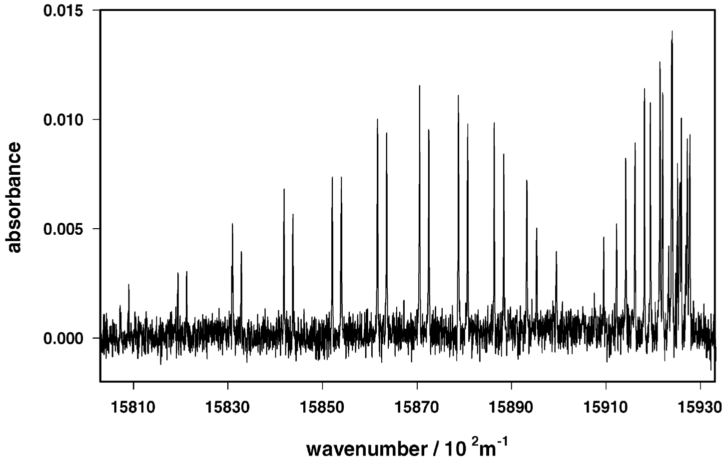

Fig. 4. Absorption spectrum of gaseous $^{16}O_2$ in the band $b\,^1\Sigma_g^+(v=2) - X\,^3\Sigma_g^-(v=0)$; length of absorption path 107 m, pressure 1.06 bar, temperature 299 K; insets show wings of the band on an expanded scale of ordinate.

component might indicate an effect of inadequate resolution on a spectrum. With knowledge of measured pressure P and temperature T of a sample, the area of each line was converted to a strength,

$$S_l = (1/N\ell)\int \ln[I_0(v)/I(v)]\,\mathrm{d}v \tag{1}$$

in which $N = N_A P/RT$ is the total number of molecules of absorbing substance per unit volume in a sample and ℓ is the length of absorbing path through a sample. Thus, effects of non-ideal gas, occupancy of vibrational states other than $X\,^3\Sigma_g^-(v=0)$ and minute presence of isotopic variants other than $^{16}O_2$ or of gaseous impurity in the sample were neglected. In practice, each spectral line was fitted according to a Lorentzian shape for which the width and stature yield an integrated area, equivalent to the integral in Eq. (1). A sum of these strengths for all lines in a band constitutes a band strength. Repeated processing of the same interferogram from the beginning proved that the reproducibility of wavenumber of each reasonably intense line was $\pm 0.01\ \mathrm{m}^{-1}$ and of width and stature $\pm 1.5\%$. Between separate recordings of the same band measured under essentially constant conditions of pressure, temperature and spectral resolution, reproducibility of wavenumber was $\pm 0.03\ \mathrm{m}^{-1}$ and of width and stature $\pm 5\%$, with these values degraded for weak lines. Standard deviations of line strengths for a given band from samples of varied density and length of absorbing path are as small as 1.5% for more intense lines in each branch, increasing to more than 50% for weak lines or lines subjected to overlap. Standard deviations of combined strengths of lines in each branch are generally about 2%, and less than that for strength of the entire band. Estimates of absolute precision of line strength, are thus generally better than 10% for an intense line, although this precision inevitably degrades for weak lines; because the latter contribute little to the integrated band strength, the relative precision of the latter is expected to be better than 10%.

3. Results

Results of our experiments consist essentially of quantitative measurements of spectra of gaseous $^{16}O_2$ in absorption at 299 K in four bands:

$$a\,^1\Delta_g(v=0) - X\,^3\Sigma_g^-(v=0)$$

and

$$b\,^1\Sigma_g^+(v=0,1,2) - X\,^3\Sigma_g^-(v=0)$$

within two specified electronic systems; the quantities measured are a wavenumber characterising each line within the rotational fine structure of each band, a full-width of each line at half-maximum stature and an area under each line. Attempts to obtain measurable absorption in other bands, specifically $a\,^1\Delta_g(v=1) - X\,^3\Sigma_g^-(v=0)$ and $b\,^1\Sigma_g^+(v=3) - X\,^3\Sigma_g^-(v=0)$, were unsuccessful within the range of length of optical path and density of sample accessible with our apparatus.

According to these measurements, the integrated intensity of each line, shift of wavenumber and width of a line are each linearly proportional to the length of optical path at constant pressure and to the density (pressure) of a sample within a tested range at a constant optical path. Hence we processed results on that basis and collect in Tables 1–4 the wavenumber (extrapolated to zero density) and mean strength of each line in separate branches of each band. In the case of overlapping lines the software allowed partition of a total contour into components of the expected number. In Table 5 we summarise band strengths and parameters for the dependence on pressure of the average shift $\Delta\nu$ and width $\delta\nu$ of lines of each band. For pressures within our range of variation the average width (full-width at half-maximum stature) was fitted to a linear relation of a form

$$\delta\nu = a + bP. \tag{2}$$

As the strength of a band is taken to be a sum of strengths of fitted lines, negligible contribution is made thereto by any prospective underlying continuum. Both the width and, to a lesser extent, the shift of a line in each band with pressure show a slight dependence on rotational quantum number R or quantum number J for total angular momentum, as exhibited by line widths in Fig. 5.

We analyzed the wavenumbers of each band, which consisted of transitions to four excited states from the state $X\,^3\Sigma_g^-(v=0)$. For the latter state we adopted values of parameters in the set valid up to $J=41$, reported by Zink and Mizushima [7], that we introduced into analytic equations to generate energies of rotational terms with relations provided by Steinbach and Gordy [8]. On a basis of these energies and wavenumbers of transitions according to Table 1 we generated rotational terms of the state $a\,^1\Delta_g(v=0)$ and fitted them to parameters in an equation

$$F(J) = \nu_0 + B_0[J(J+1) - \Lambda^2] - D_0[J(J+1) - \Lambda^2]^2 \tag{3}$$

with $\Lambda = 2$ appropriate for this state; deduced values of band parameters appear in Table 6.

Likewise for three bands of the system $b - X$ we generated rotational terms from which band parameters in Table 7 are deduced. To derive meaningful values of term coefficients Y_{k1} in this table we included parameters of the band $b\,^1\Sigma_g^+ v'=3 - X\,^3\Sigma_g^- v''=0$ from an analysis, according to the same procedure as that applied to the bands $b\,^1\Sigma_g^+ v'=0,1,2 - X\,^3\Sigma_g^- v''=0$ measured in this work, of wavenumbers of the former band reported by Biennier and Campargue [9].

Table 1
Wavenumbers and strengths of lines of $^{16}O_2$ in the band $a\,^1\Delta_g(v=0) - X\,^3\Sigma_g^-(v=0)$ at 299 K[a]

Line	$\tilde{\nu}$ (m^{-1})	S_l (10^{-28} m)	Line	$\tilde{\nu}$ (m^{-1})	S_l (10^{-28} m)	Line	$\tilde{\nu}$ (m^{-1})	S_l (10^{-28} m)
						^{r}Q(1)	788995.24	1.86
			^{q}P(3)	788415.67	0.93	^{r}Q(3)	789549.86	4.02
^{o}P(5)	785834.33	0.76	^{q}P(5)	788386.40	3.63	^{r}Q(5)	790084.68	5.52
^{o}P(7)	784645.39	1.29	^{q}P(7)	788335.00	2.27	^{r}Q(7)	790602.40	6.29
^{o}P(9)	783442.21	1.76	^{q}P(9)	788269.78	1.46	^{r}Q(9)	791103.39	6.40
^{o}P(11)	782224.13	1.79	^{q}P(11)	788187.04	2.51	^{r}Q(11)	791587.64	5.78
^{o}P(13)	780991.26	1.49	^{q}P(13)	788090.88	1.68	^{r}Q(13)	792055.14	4.68
^{o}p(15)	779743.79	1.34	^{q}P(15)	787978.47	3.90	^{r}Q(15)	792505.78	3.67
^{o}P(17)	778481.66	1.02	^{q}P(17)	787847.20	0.95	^{r}Q(17)	792939.39	2.65
^{o}P(19)	777204.75	0.62	^{q}P(19)	787700.63	0.55	^{r}Q(19)	793355.86	1.61
^{o}P(21)	775913.85	0.36	^{q}P(21)	787538.45	0.42	^{r}Q(21)	793754.94	1.01
^{o}P(23)	774608.26	0.24	^{q}P(23)	787359.32	0.30	^{r}Q(23)	794136.44	0.59
^{o}P(25)	773288.16	0.18	^{q}P(25)	787166.10	0.17	^{r}Q(25)	794499.95	0.27
						^{r}Q(27)	794847.48	0.16
						^{r}R(1)	788807.63	6.69
^{p}P(3)	787370.31	0.78	^{q}Q(3)	788220.65	5.96	^{r}R(3)	789354.84	7.82
^{p}P(5)	786767.29	2.12	^{q}Q(5)	788184.84	10.27	^{r}R(5)	789885.95	8.54
^{p}P(7)	786149.01	3.24	^{q}Q(7)	788133.25	10.91	^{r}R(7)	790400.83	8.64
^{p}P(9)	785515.13	3.74	^{q}Q(9)	788065.77	11.14	^{r}R(9)	790899.38	7.96
^{p}P(11)	784865.67	3.80	^{q}Q(11)	787982.20	9.69	^{r}R(11)	791381.48	7.05
^{p}P(13)	784200.66	3.15	^{q}Q(13)	787882.53	8.67	^{r}R(13)	791846.97	5.35
^{p}P(15)	783520.21	2.74	^{q}Q(15)	787766.88	6.37	^{r}R(15)	792295.64	4.05
^{p}P(17)	782824.42	1.84	^{q}Q(17)	787634.98	4.61	^{r}R(17)	792727.26	2.80
^{p}P(19)	782112.97	1.37	^{q}Q(19)	787486.86	3.26	^{r}R(19)	793141.88	1.90
^{p}P(21)	781386.45	0.77	^{q}Q(21)	787322.17	2.10	^{r}R(21)	793539.08	1.14
^{p}P(23)	780644.21	0.50	^{q}Q(23)	787141.32	1.25	^{r}R(23)	793918.92	0.76
^{p}P(25)	779886.65	0.32	^{q}Q(25)	786944.14	0.72	^{r}R(25)	794280.88	0.51
^{p}P(27)	779113.99	0.08	^{q}Q(27)	786729.64	0.35	^{r}R(27)	794624.82	0.21
			^{q}Q(29)	786500.17	0.18	^{r}R(29)	794950.50	0.08
						^{s}R(1)	789846.09	3.49
^{p}Q(3)	787578.56	1.61	^{q}R(3)	788429.02	3.57	^{s}R(3)	790967.46	4.23
^{p}Q(5)	786968.55	3.81	^{q}R(5)	788384.63	1.72	^{s}R(5)	792069.02	4.67
^{p}Q(7)	786346.40	4.92	^{q}R(7)	788331.16	3.28	^{s}R(7)	793153.08	4.59
^{p}Q(9)	785709.68	5.24	^{q}R(9)	788260.24	3.74	^{s}R(9)	794219.93	4.29
^{p}Q(11)	785057.81	4.80	^{q}R(11)	788174.31	3.45	^{s}R(11)	795269.49	3.77
^{p}Q(13)	784390.72	4.27	^{q}R(13)	788072.53	2.50	^{s}R(13)	796301.78	2.92
^{p}Q(15)	783708.27	3.15	^{q}R(15)	787954.94	1.98	^{s}R(15)	797316.35	2.11
^{p}Q(17)	783010.52	2.31	^{q}R(17)	787820.88	1.51	^{s}R(17)	798313.19	1.51
^{p}Q(19)	782297.24	1.64	^{q}R(19)	787670.93	0.87	^{s}R(19)	799291.78	1.00
^{p}Q(21)	781568.59	1.02	^{q}R(21)	787505.24	0.76	^{s}R(21)	800252.27	0.65
^{p}Q(23)	780824.88	0.62	^{q}R(23)	787322.63	0.54	^{s}R(23)	801193.14	0.40
^{p}Q(25)	780065.87	0.25	^{q}R(25)	787123.19	0.20	^{s}R(25)	802116.13	0.17
^{p}Q(27)	779290.66	0.30				^{s}R(27)	803017.16	0.19

[a] Severe overlap of lines in the following sets P(3) and ^{q}R(3); ^{q}P(5) and ^{q}R(5); ^{q}P(11), ^{q}Q(5) and ^{q}R(11); ^{q}P(15) and ^{q}Q(11); ^{q}Q(9) and ^{q}R(13) precludes accurate empirical partition of total intensity of a composite feature to specified individual transitions.

Table 2
Wavenumbers and strengths of lines of $^{16}O_2$ in the band $b\,^1\Sigma_g^+(v=0) - X\,^3\Sigma_g^-(v=0)$ at 299 K

Line	$\tilde{\nu}$ (m^{-1})	S_l (10^{-27} m)	Line	$\tilde{\nu}$ (m^{-1})	S_l (10^{-27} m)
$^PP(1)$	1311804.40	25.7	$^rQ(1)$	1312826.85	30.1
$^PP(3)$	1311201.44	49.4	$^rQ(3)$	1313343.98	53.1
$^PP(5)$	1310561.53	65.7	$^rQ(5)$	1313820.26	69.2
$^PP(7)$	1309884.68	73.3	$^rQ(7)$	1314258.07	74.6
$^PP(9)$	1309170.89	72.1	$^rQ(9)$	1314657.76	72.5
$^PP(11)$	1308420.22	64.4	$^rQ(11)$	1315019.31	66.6
$^PP(13)$	1307632.58	53.2	$^rQ(13)$	1315342.74	52.6
$^PP(15)$	1306808.04	41.3	$^rQ(15)$	1315627.66	41.9
$^PP(17)$	1305946.53	29.2	$^rQ(17)$	1315871.17	28.9
$^PP(19)$	1305047.93	15.2	$^rQ(19)$	1316081.28	17.2
$^PP(21)$	1304112.20	12.2	$^rQ(21)$	1316248.92	7.9
$^PP(23)$	1303139.20	7.2	$^rQ(23)$	1316377.98	7.0
$^PP(25)$	1302128.92	3.7	$^rQ(25)$	1316467.15	4.4
$^PP(27)$	1301080.87	2.0	$^rQ(27)$	1316515.66	
$^PP(29)$	1299996.54	0.9	$^rQ(29)$	1316524.26	
$^PP(31)$	1298872.44	0.5			
			$^rR(1)$	1312639.20	12.8
$^PQ(3)$	1311409.90	34.8	$^rR(3)$	1313149.01	37.2
$^PQ(5)$	1310762.71	51.7	$^rR(5)$	1313621.53	54.2
$^PQ(7)$	1310082.03	61.7	$^rR(7)$	1314056.48	61.9
$^PQ(9)$	1309365.41	64.0	$^rR(9)$	1314453.77	64.2
$^PQ(11)$	1308612.39	58.2	$^rR(11)$	1314813.25	60.2
$^PQ(13)$	1307822.62	49.2	$^rR(13)$	1315134.50	50.9
$^PQ(15)$	1306996.07	38.0	$^rR(15)$	1315417.60	37.4
$^PQ(17)$	1306132.63	27.7	$^rR(17)$	1315661.99	25.0
$^PQ(19)$	1305232.14	18.6	$^rR(19)$	1315873.33	16.7
$^PQ(21)$	1304294.55	11.6	$^rR(21)$	1316034.02	12.5
$^PQ(23)$	1303319.76	7.0	$^rR(23)$	1316160.75	5.1
$^PQ(25)$	1302307.76	3.5	$^rR(25)$	1316252.21	4.6
$^PQ(27)$	1301258.33	1.9	$^rR(27)$	1316293.33	2.0
$^PQ(29)$	1300169.24	1.1	$^rR(29)$	1316298.89	0.7
$^PQ(31)$	1299045.93	0.6			

4. Discussion

We discuss in turn the wavenumbers, strengths, shifts and widths of lines in each band individually.

4.1. $a^1\Delta_g(v=0) - X^3\Sigma_g^-(v=0)$

The wavenumbers of these lines in Table 1 are $0.77 \pm 0.17\ m^{-1}$ greater than those reported by Amiot and Verges [10]. The spectral parameters in columns a and b in Table 6 differ primarily

Table 3
Wavenumbers and strengths of lines of $^{16}O_2$ in the band $b\,^1\Sigma_g^+(v=1) - X\,^3\Sigma_g^-(v=0)$ at 299 K

Line	$\tilde{\nu}$ (m^{-1})	S_l (10^{-27} m)	Line	$\tilde{\nu}$ (m^{-1})	S_l (10^{-27} m)
$^pP(1)$	1452278.19	1.96	$^rQ(1)$	1453289.71	2.41
$^pP(3)$	1451664.13	3.79	$^rQ(3)$	1453781.16	4.28
$^pP(5)$	1450998.59	5.05	$^rQ(5)$	1454217.28	5.58
$^pP(7)$	1450281.50	5.65	$^rQ(7)$	1454600.20	6.12
$^pP(9)$	1449512.88	5.59	$^rQ(9)$	1454930.47	5.91
$^pP(11)$	1448692.66	4.98	$^rQ(11)$	1455208.03	5.54
$^pP(13)$	1447820.90	4.15	$^rQ(13)$	1455432.66	3.37
$^pP(15)$	1446897.54	3.20	$^rQ(15)$	1455603.90	3.38
$^pP(17)$	1445922.56	2.33	$^rQ(17)$	1455722.13	2.54
$^pP(19)$	1444895.87	1.58	$^rQ(19)$	1455787.08	1.74
$^pP(21)$	1443817.27	0.98	$^rQ(21)$	1455797.00	0.83
$^pP(23)$	1442686.78	0.59	$^rQ(23)$	1455754.21	0.59
$^pP(25)$	1441504.05	0.32	$^rQ(25)$	1455655.65	0.37
$^pP(27)$	1440269.46	0.17	$^rQ(27)$	1455502.84	0.21
$^pP(29)$	1438982.08	0.07	$^rQ(29)$	1455297.42	0.09
			$^rR(1)$	1453101.85	1.11
$^pQ(3)$	1451872.64	2.63	$^rR(3)$	1453586.31	2.81
$^pQ(5)$	1451199.78	4.01	$^rR(5)$	1454018.49	4.35
$^pQ(7)$	1450478.88	4.87	$^rR(7)$	1454398.53	5.09
$^pQ(9)$	1449707.45	5.09	$^rR(9)$	1454726.44	5.36
$^pQ(11)$	1448884.81	4.67	$^rR(11)$	1455001.82	4.51
$^pQ(13)$	1448010.94	3.96	$^rR(13)$	1455224.41	3.67
$^pQ(15)$	1447085.59	3.04	$^rR(15)$	1455393.79	3.20
$^pQ(17)$	1446108.67	2.26	$^rR(17)$	1455510.31	2.57
$^pQ(19)$	1445080.04	1.50	$^rR(19)$	1455573.00	1.76
$^pQ(21)$	1443999.67	0.96	$^rR(21)$	1455581.65	0.85
$^pQ(23)$	1442867.54	0.55	$^rR(23)$	1455536.48	0.71
$^pQ(25)$	1441683.04	0.35	$^rR(25)$	1455430.49	0.42
$^pQ(27)$	1440446.44	0.16	$^rR(27)$	1455284.16	0.11
$^pQ(29)$	1439158.26	0.08			

because in their fit the subtrahend Λ^2 was excluded from Eq. (3), and likewise for the analysis by Herzberg and Herzberg [1]. When we also fitted without that subtrahend, our values of the parameters were similar, within a few standard errors, to those of earlier workers. Furthermore, in such a fit H_0 assumed an almost significant value, whereas with Λ^2 taken into account no such significance arose; therefore the apparent significance of H_0 deduced by Amiot and Verges [10] may be an artifact of their procedure, especially as the extent of their rotational excitation was appreciably less than in our spectra. Agreement with spectral parameters deduced from fitting reported frequencies of pure rotational transitions [11] within the state $a\,^1\Delta_g(v=0)$ up to $J''=9$ is also satisfactory; although parameters from the latter fit are more precise than ours, reflecting correspondingly much more precise measurements of frequencies of transitions [11]; they

Table 4
Wavenumbers and strengths of lines of $^{16}O_2$ in the band $b\,^1\Sigma_g^+(v=2) - X\,^3\Sigma_g^-(v=0)$ at 299 K

Line	$\tilde{\nu}$ (m^{-1})	S_l (10^{-28} m)	Line	$\tilde{\nu}$ (m^{-1})	S_l (10^{-28} m)
$^pP(1)$	1589954.23	0.82	$^rQ(1)$	1590955.80	0.93
$^pP(3)$	1589330.63	1.45	$^rQ(3)$	1591421.37	1.62
$^pP(5)$	1588639.53	2.04	$^rQ(5)$	1591816.90	2.21
$^pP(7)$	1587881.70	2.32	$^rQ(7)$	1592144.30	2.53
$^pP(9)$	1587058.10	2.29	$^rQ(9)$	1592405.73	2.19
$^pP(11)$	1586167.87	1.98	$^rQ(11)$	1592598.17	2.07
$^pP(13)$	1585211.67	1.68	$^rQ(13)$	1592723.33	1.69
$^pP(15)$	1584189.33	1.21	$^rQ(15)$	1592780.07	1.20
$^pP(17)$	1583100.00	0.89	$^rQ(17)$	1592771.60	1.14
$^pP(19)$	1581945.63	0.59	$^rQ(19)$	1592691.10	0.61
$^pP(21)$	1580726.15	0.45	$^rQ(21)$	1592544.30	0.34
			$^rR(1)$	1590764.00	0.34
$^pQ(3)$	1589538.17	1.04	$^rR(3)$	1591227.27	1.29
$^pQ(5)$	1588840.40	1.67	$^rR(5)$	1591617.47	1.68
$^pQ(7)$	1588078.73	1.97	$^rR(7)$	1591943.60	2.18
$^pQ(9)$	1587252.57	1.96	$^rR(9)$	1592201.67	2.09
$^pQ(11)$	1586360.47	1.86	$^rR(11)$	1592393.40	2.06
$^pQ(13)$	1585401.90	1.57	$^rR(13)$	1592515.13	1.69
$^pQ(15)$	1584377.80	1.08	$^rR(15)$	1592571.07	1.23
$^pQ(17)$	1583286.13	0.93	$^rR(17)$	1592559.20	1.14
$^pQ(19)$	1582126.80	0.53	$^rR(19)$	1592477.60	0.72
$^pQ(21)$	1580906.75	0.40	$^rR(21)$	1592329.27	0.68
			$^rR(23)$	1592108.71	0.31

Table 5
Strengths of bands, average shifts and parameters a and b characterizing widths of lines of $^{16}O_2$ as a function of pressure at 299 K

Band	S_b (10^{-27} m)	$\Delta\tilde{\nu}$ (m^{-1} bar^{-1})	a (m^{-1})	b (m^{-1} bar^{-1})
$a\,^1\Delta_g(v=0) - X\,^3\Sigma_g^-(v=0)$	32.47 ± 0.80	-0.35 ± 0.16	2.7 ± 0.2	7.8 ± 0.5
$b\,^1\Sigma_g^+(v=0) - X\,^3\Sigma_g^-(v=0)$	1921 ± 23	-1.10 ± 0.25	3.6 ± 0.2	6.9 ± 0.24
$b\,^1\Sigma_g^+(v=1) - X\,^3\Sigma_g^-(v=0)$	154.6 ± 2.4	-1.1 ± 0.45	3.5 ± 0.7	7.4 ± 1.0
$b\,^1\Sigma_g^+(v=2) - X\,^3\Sigma_g^-(v=0)$	6.08 ± 0.38	-3.8 ± 1.2	5.7 ± 0.5	8.3 ± 0.6

reproduce frequencies involving rotational energies up to only $J = 10$, whereas our parameters reproduce rotational energies in the state $a\,^1\Delta_g(v=0)$ up to $J = 29$.

For this band near 7.9×10^5 m^{-1} a band strength $(3.25 \pm 0.08) \times 10^{-26}$ m in Table 5 is comparable with 3.5×10^{-26} m (with no indication of uncertainty) that Badger et al. [12] deduced from measurements of the same band in absorption with a grating spectrometer, optical path of length 32 m and spectral resolution 25 m^{-1}; for comparison the length of our absorbing path for most

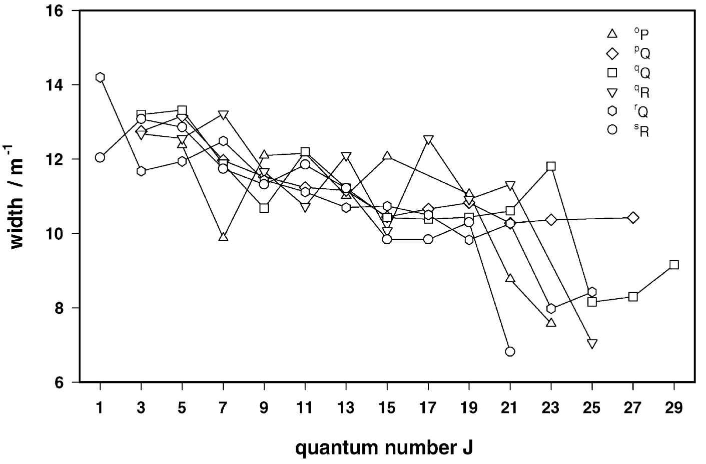

Fig. 5. Widths of spectral lines of gaseous $^{16}O_2$ in branches of the band $a\,^1\Delta_g(v=0) - X\,^3\Sigma_g^-(v=0)$; experimental conditions are the same as in Fig. 1.

Table 6
Spectral parameters/m^{-1} of $^{16}O_2$ in the state $a\,^1\Delta_g(v=0)$

	This work[a]	Amiot/Verges (Ref. [10])	Herzberg/Herzberg (Ref. [1])	Cohen et al.[b] (Ref. [11])
$\tilde{\nu}_{0-0}$	788810.7842 ± 0.0086	788376.179 ± 0.028[c,d]	788239[c]	
B_0	141.780381 ± 0.000090	141.784020 ± 0.000082	141.783	141.7798053 ± 0.0000075
D_0 (10^{-4})	5.11144 ± 0.00139	5.1769 ± 0.0056		5.09830 ± 0.00165
H_0 (10^{-10})		1.589 ± 0.098		− 0.244 ± 0.101
$\tilde{\sigma}_{0-0}$	0.021			0.000058

[a] $\tilde{\sigma}_{0-0}$ implies a standard deviation of a fit; each uncertainty indicates a single standard error.
[b] Fitted from frequencies reported by Cohen et al. [11], including H_0 rather than q_0 within the set of parameters yielded a superior fit.
[c] Obtained from fitting excluding Λ^2; see text.
[d] Origins relative to $F_3(R=1, J=0)$ in $X\,^3\Sigma_g^-$; an offset − 133.159 m^{-1} is applicable (see text).

measurements was 85.25 m and the resolution was 2.5 m^{-1}. Thus, whereas Badger et al. [12] comment on their poorly resolved lines, our lines are successfully resolved, except cases with severe overlap near the band center, as the effective resolution was much less than the widths of lines, even at the smallest densities of our samples. Unlike experiments of Badger et al. [12] our measurements exclude any significant component of underlying continuum due to absorption of complexes $(O_2)_2$, of which a contribution to total intensity would be in any case negligible at our smallest densities of sample. Lafferty et al. report [13] a value $(3.182 \pm 0.069) \times 10^{-26}$ m at 296 K based on measurements made under conditions similar to ours but with an alternative method of analysis based on only 54 lines with $J = 23$ maximum, but generally less, in any branch. In contrast, our sum of line

Table 7
Spectral parameters/m^{-1} of $^{16}O_2$ in the system $b\,^1\Sigma_g^+ - X\,^3\Sigma_g^-$

	This work[a]	Phillips et al. (Ref. [12])	Kanamori et al. (Ref. [13])	Babcock/Herzberg (Ref. [14])
$\tilde{\nu}_{0-0}$	1312091.8775 ± 0.0125	1312224.08 ± 0.03[b]	1312225.27 ± 0.05[b]	1312090.80
B_0	139.124421 ± 0.000178	139.1255 ± 0.0003	139.1249 ± 0.0003	139.132
D_0 (10^{-4})	5.3641 ± 0.0021	5.385 ± 0.008	5.373 ± 0.003	5.39
$\tilde{\sigma}_{0-0}$	0.038			
$\tilde{\nu}_{1-0}$	1452565.553 ± 0.026	1452699.76 ± 0.12[e]		1452566.02
B_1	137.29659 ± 0.00022	137.2951 ± 0.0018		137.3054
D_1 (10^{-4})	5.4086 ± 0.0042	5.397 ± 0.050		5.458
$\tilde{\sigma}_{1-0}$	0.043			
$\tilde{\nu}_{2-0}$	1590242.51 ± 0.32			1590241.56
B_2	135.4644 ± 0.0038			135.4731
D_2 (10^{-4})	5.540 ± 0.077			5.567
$\tilde{\sigma}_{2-0}$	0.50			
T_e	1319515.86 ± 0.21			1319522.21
$Y'_{1,0}$	143273.38 ± 0.49			143268.74
$Y'_{2,0}$	− 1399.84 ± 0.22			− 1395.008
$Y'_{0,1}$	140.03506 ± 0.00036			140.0416
$Y'_{1,1}$	− 1.81910 ± 0.00084			− 1.8170
$Y'_{2,1}$ (10^{-3})	− 4.35 ± 0.40			− 4.3
$Y'_{0,2}$ (10^{-4})	− 5.3417 ± 0.0019			− 5.356
$Y'_{1,2}$ (10^{-6})	− 4.48 ± 0.24			− 7.7

[a] $\tilde{\sigma}_{v'-0}$ implies a standard deviation of a fit of a particular band.
[b] Origins relative to $F_3(R = 1, J = 0)$ in $X\,^3\Sigma_g^-$; an offset − 133.159 m^{-1} is applicable (see text).

strengths to constitute the band strength includes 118 lines up to at least $J = 25$ in every branch, and generally greater until further lines essentially vanished below the noise level; any contribution from excluded lines is estimated to be less than 0.2% of the total band strength. The fractions of total band strength in each branch according to Table 1 are closely similar to values reported by Lafferty et al. [13]. Even though overlapping lines might not have their contributions to intensity partitioned accurately to a particular branch, the band strength as total intensity is unaffected in this way. These three results for band strength are likely not in real discord, but reflect varied methods of collecting and processing spectral data. Our present value has a precision considerably improved relative to our previous values [3], as a result of the greater length of absorbing path of sample and improved processing of data. Problems with overlapping lines in branches ^qP, ^qQ and ^qR remain, however, and are unlikely to be resolved by means of measurements of absorption for samples in which widths of lines reflect collisional broadening.

Although in Table 5 we present an average value of widths of lines in this band, Fig. 5 demonstrates that, for six of the nine branches of this band for which lines were subject to little interference or overlap, the width decreases about a third as R or J increases in the range [1,27]. Similar trends were discernible in widths of lines in measured bands in the other electronic system. The intercept on the ordinate axis of a plot of width of line versus pressure is slightly greater than the spectral

Table 8
Strengths/10^{-27} m of selected lines of $^{16}O_2$ in the band $b\,^1\Sigma_g^+(v=0) - X\,^3\Sigma_g^-(v=0)$

Line	This work 299 K	Ray and Ghosh [33] 300 K	Ritter and Wilkerson [21] 294 K	Miller et al. [18] 293 K
$^PP(1)$	25.7 ± 0.5		31.6 ± 0.5	26.4 ± 2.2
$^PQ(7)$	61.7 ± 0.4		72.8 ± 0.3	62.5 ± 3.6
$^PP(7)$	73.3 ± 1.3		86.5 ± 0.9	75.1 ± 3.4
$^rQ(11)$	66.6 ± 1.0		78.2 ± 1.3	67.4 ± 3.3
$^rR(11)$	60.2 ± 1.8		69.1 ± 0.5	67.4 ± 3.3
$^rR(13)$	50.9 ± 2.0		57.4 ± 0.3	49.0 ± 2.0
$^rQ(19)$	17.2 ± 1.9	17.3 ± 1.8	22.5 ± 0.1	
$^rR(21)$	12.5 ± 1.6	10.20 ± 0.16	12.9 ± 0.1	
$^rQ(23)$	7.0 ± 2.0	14.8 ± 0.7	8.08 ± 0.11	
$^rR(23)$	5.1 ± 1.1	9.23 ± 0.05	7.61 ± 0.17	

resolution, consistent with a convolution of that value with the dopplerian width 1.7 m^{-1} at the temperature of these measurements. The average width of lines at a pressure 1 bar is 10.5 ± 0.6 m^{-1} (as the sum, for that pressure, of a and b in Table 5), in agreement with the mean width 10.24 ± 0.71 m^{-1} reported by Lafferty et al. [13] at that pressure. In contrast the shift of wavenumber with pressure is barely significant. Although diode lasers are likely to provide a method for measuring the width of spectral lines superior to that with an interferometer, to measure thus strengths and absolute wavenumbers of lines or their shifts with pressure is more difficult.

We expended considerable effort to detect the band $a\,^1\Delta_g(v=1) - X\,^3\Sigma_g^-(v=0)$ but found no trace of it. We thus estimate only an upper limit 1×10^{-29} m for a strength of any intense line in that band; a corresponding upper limit of band strength would be 3×10^{-28} m.

4.2. $b^1\Sigma_g^+(v=0) - X^3\Sigma_g^-(v=0)$

The wavenumbers of lines listed in Table 2, calibrated and corrected for pressure shift, are larger than those reported by Babcock and Herzberg [14] by about 1 m^{-1} for all four branches; discrepancies are likely to be within combined uncertainties of measurement, especially as the latter data were measured for an atmospheric sample. Comparison of spectral parameters in Table 7 indicates that our data are significantly more precise than any previously reported. Omitted from Table 7 are parameters published by Albritton et al. [15] that are derived from reanalysis of data of Babcock and Herzberg [14] and that have values similar to, but precision inferior to, those reported by Kanamori et al. [16]. The origins of all three bands in this system are relative to the existing rotational state $F_3(R=1, J=0)$ of least energy in $X\,^3\Sigma_g^-(v=0)$; the differences between $\tilde{\nu}_{v-0}$ with this convention in Table 7 and others from the literature correspond to $2\lambda_0/3 - \gamma_0 \approx 133.159$ m^{-1}.

Strengths of selected lines are compared in Table 8 with published data; agreement is satisfactory. Ratios of our measured intensities of this band are consistent with theoretical Honl-London factors (which are $(J+1)/2$ for the branch ^{P}P and $J/2$ for the branch ^{r}R, with more complicated expressions for the other two branches [17]) and Boltzmann factors. Our band strength

1.92×10^{-24} m is basically consistent with values/10^{-24} m of Miller et al. [18], 1.98; of Galkin et al. [19], 1.87, and of Grossman (Ref. [20], reported in Ref. [21]), 1.97; but not of Cho et al. [22], 2.14; of Burch and Gryvnak [23], 2.18; of Wallace and Hunten [24], 2.11; of Adiks and Dianov-Klokov [25,26], 2.11; of Ritter and Wilkerson [21], 2.28 ± 0.04; of Childs and Mecke [27], 3.02; of Allen [28], 1.57 (atmosphere) and 1.54 (laboratory); of de Jager [29], 2.53; of Wark and Mercer (Refs. [30,31], corrected in Ref. [24]), 2.72, and of van de Hulst [32], 4.83.

Our mean widths of lines for self-broadening of O_2 at pressure 1 bar, $(10.5\pm0.3)\ \mathrm{m}^{-1}$ according to data in Table 5, are comparable with those reported by Ritter and Wilkerson [21], by Miller et al. [18] and by Ray and Ghosh [33]. Our mean shifts, $-1.10\ \mathrm{m}^{-1}\ \mathrm{bar}^{-1}$, agree with those reported by Phillips and Hamilton [34], but have a magnitude slightly larger than that, $0.81\ \mathrm{m}^{-1}\ \mathrm{bar}^{-1}$, mentioned by Kessler et al. [35]:

4.3. $b^1\Sigma_g^+(v=1)-X^3\Sigma_g^-(v=0)$

As for the preceding band, our wavenumbers agree closely with those reported by Babcock and Herzberg [14], but origins of both bands disagree with those reported by Phillips et al. [36], for a reason mentioned above. Rotational and centrifugal-distortion parameters among the three sets agree satisfactorily, with our results being again the most precise.

We can compare our line strengths in Table 3 as values/10^{-27} m for the line $^{\mathrm{r}}$R(11), 4.51, with those of Fiegel et al. [37], 4.6, of Giver et al. [38], 4.43, and that, 3.7, quoted by Fiegel et al. from a large compilation [39], and for the line $^{\mathrm{p}}$P(7), 5.65, compared with that from Giver et al. [38], 5.70, and their quoted value 4.6 from a compilation [39]. Our ratios of intensities conform to those expected on a basis of Honl-London and Boltzmann factors as a theoretical model incorporating neither vibration-rotational nor electronic-rotational interaction. Our value/10^{-25} m of the band strength, 1.55, is thus comparable with values of Galkin et al. [19], 1.40, and of Giver et al. [38], 1.67, but different from those of Childs and Mecke [27], 2.96, of Allen [28], 1.27 and of van de Hulst [32], 2.33.

Our measured shift of wavenumbers with pressure of gaseous O_2, in Table 5, is the same for this band as for the band $b\,^1\Sigma_g^+(v=0)-X\,^3\Sigma_g^-(v=0)$, but with a larger standard error; within that uncertainty our value/$\mathrm{m}^{-1}\,\mathrm{bar}^{-1}$ agrees with two values previously reported, an average (-1.4 ± 0.4) for the entire band [36] and (-0.79 ± 0.02) for a line $^{\mathrm{r}}$R(11) [37]. Likewise for widths of separate rotational lines in these two bands to $v'=0$ and 1, the characteristics are similar; larger standard errors attached to parameters reflect a decreased ratio of signal to noise of measurements of the latter band. Our mean value $b=(7.4\pm1.0)\ \mathrm{m}^{-1}\ \mathrm{bar}^{-1}$ for all lines is about half the value $b=(12.5\pm1.1)$ deduced for $^{\mathrm{r}}$R(11) alone from plots by Fiegel et al. [37] and our mean width $(10.9\pm1.2)\ \mathrm{m}^{-1}$ at 1 bar is intermediate between the extrema 12.8 m^{-1} at $J=1$ and 8.4 m^{-1} at $J=25$ reported by Giver et al. [38].

4.4. $b^1\Sigma_g^+(v=2)-X^3\Sigma_g^-(v=0)$

For comparison with our results for wavenumbers of lines in this band in Tables 4 and 7 there are only data reported by Babcock and Herzberg [14]. The wavenumbers listed in Table 4 are on average $(1.11\pm0.23)\ \mathrm{m}^{-1}$ greater than in the earlier list, which constitutes satisfactory agreement within combined uncertainties of measurements, and parameters of this band agree similarly.

Relative strengths of these lines in Table 4 conform reasonably well to ratios expected on the basis of populations of rotational states within $X\,^3\Sigma_g^-(v=0)$ and Honl-London factors (which are common to all bands of this system). Because net absorbances of lines in this band are small, producing only moderate ratios of signal to noise even under our conditions of maximum practicable pressure of sample and maximum length of absorbing path, relative standard deviations of line strengths are larger than for other bands reported here, ranging from at least 3% for more intense lines in each branch to as much as 38% for the weakest lines; overlap of lines near heads in branches ^rQ and ^rR also contributes to uncertainties of strength of lines listed in Table 4.

No other direct measurements of widths or shifts of lines in this band are known, but our estimate of mean shift in Table 5 is larger than those of bands to $v'=0$ and 1, and the magnitude is also larger than an indirect estimate $-0.77\ m^{-1}$ from modeling of asymmetry [40]. In Table 5 the value of a for this band reflects worse resolution, $6\ m^{-1}$, that prevailed during measurement of this band because the intensity is small.

We tried but failed to detect the band $b\,^1\Sigma_g^+ v'=3-X\,^3\Sigma_g^- v''=0$. Our estimated upper limit of band strength on the basis of such attempts would be approximately the same as that for the band $a\,^1\Delta_g v'=1-X\,^3\Sigma_g^- v''=0$, namely 3×10^{-28} m; this value is comparable with the band strength deduced by Biennier and Campargue [9], namely 1.8×10^{-28} m.

5. Conclusion

We present results of measurements of characteristics of lines in four bands belonging to two systems in the electronic spectrum of gaseous O_2 that have small strengths, consistent with their electronic transition moments involving mostly a magnetic dipole rather than an electric dipole. The band $b\,^1\Sigma_g^+(v=2)-X\,^3\Sigma_g^-(v=0)$ is the weakest for which quantitative measurements of line strengths are practicable in this laboratory under present conditions. Because these strengths are so small, there are conspicuous experimental difficulties involved in undertaking these measurements, but comparison with published results provides satisfactory confirmation of the accuracy of our approach. For this reason our results can serve as a reliable basis of modeling radiative properties of the terrestrial atmosphere. Results presented in Tables 1–7 are significantly improved over those adopted for the purpose of preparation of the HITRAN database (1996) [41].

Acknowledgements

We thank Professor J.W. Nibler at Oregon State University and Professor J.C.A. Boeyens at University of the Witwatersrand for hospitality to JFO during analysis of our data, and National Science Council of Republic of China (Taiwan) for financial support of this research (grant No. NSC88-2119-M-007-001).

References

[1] Herzberg L, Herzberg G. Astrophys J 1947;105:353–9.
[2] Mlynczak MG, Marshall BT. Geophys Res Lett 1996;23:657–60.

[3] Hsu YT, Lee Y-P, Ogilvie JF. Spectrochim Acta 1992;A48:1227–30.
[4] Mills IM. Quantities, units and symbols in physical chemistry, rev. ed., IUPAC, Oxford, UK: Blackwell Scientific, 1992.
[5] Phelps III FM. M. I. T. wavelength tables, vol. 2. Massachusetts, USA: MIT Press, 1982.
[6] Gerstenkorn S, Luc P. Atlas du Spectre d'Absorption de la Molecule d'Iode. Paris, France: Editions du Centre National de la Recherche Scientifique, 1978.
[7] Zink LR, Mizushima M. J Mol Spectrosc 1987;125:154–8.
[8] Steinbach W, Gordy W. Phys Rev 1973;A8:1753–8.
[9] Biennier L, Campargue A. J Mol Spectrosc 1998;188:248–50.
[10] Amiot C, Verges J. Can J Phys 1981;59:1391–8.
[11] Cohen EA, Okunishi M, Oh JJ. J Mol Struct 1995;352:283–7.
[12] Badger RM, Wright AC, Whitlock RF. J Chem Phys 1965;43:4345–50.
[13] Lafferty WJ, Solodov AM, Lugez CL, Fraser GT. Appl Opt 1998;37:2264–70.
[14] Babcock HD, Herzberg L. Astrophys J 1948;108:167–90.
[15] Albritton DL, Harrop WJ, Schmeltekopf AL, Zare RN. J Mol Spectrosc 1973;46:103–18.
[16] Kanamori H, Momona M, Sakurai K. Can J Phys 1990;68:313–6.
[17] Watson JKG. Can J Phys 1968;46:1637–43.
[18] Miller JH, Boese RW, Giver LP. JQSRT 1969;9:1507–17.
[19] Galkin VD, Shukova LN, Mitrofanova LA. Optika i Spektroskopia 1972;33:837–43; Opt Spectrosc 1973;35:367–70.
[20] Grossman B. Etude par spectroscopie d'absorption laser en regime continu et impulsionnel des molecules d'eau et d'oxygene. Doctoral thesis, University Pierre and Marie Curie, 1984, reported in Ref. [21].
[21] Ritter KJ, Wilkerson TD. J Mol Spectrosc 1987;121:1–19.
[22] Cho CW, Allin EJ, Welsh HJ. Can J Phys 1968;41:1993–2002.
[23] Burch DE, Gryvnak DA. Appl Opt 1969;8:1493–9.
[24] Wallace L, Hunten DM. J Geophys Res 1968;73:4813–34.
[25] Adiks TG, Dianov-Klokov VI. Izv Akad Nauka SSSR, Fiziki Atmosfira i Ozhiana 1968;4:1052–9.
[26] Adiks TG, Dianov-Klokov VI. Opt Spektrosk 1972;32:432–3.
[27] Childs WHJ, Mecke R. Z Phys 1931;68:344–61.
[28] Allen CW. Astrophys J 1937;85:156–64.
[29] de Jager D. Bull Astron Soc Neth XIII 1956;467:9–17.
[30] Wark DQ, Mercer DM. Appl Opt 1965;4:839–45.
[31] Wark DQ, Mercer DM. Appl Opt 1966;5:1469.
[32] van de Hulst HC. Ann Astrophys 1945;8:12–23.
[33] Ray B, Ghosh PN. Spectrochim Acta 1997;A53:537–43.
[34] Phillips AJ, Hamilton PA. J Mol Spectrosc 1995;174:587–94.
[35] Kessler WJ, Davis SJ, Hunter AJR. Interdisplinary Laser Sciences — XII, abstract ThC4, Rochester, New York, USA, 1996.
[36] Phillips AJ, Peters F, Hamilton PA. J Mol Spectrosc 1997;184:162–6.
[37] Fiegel RP, Hays PB, Wright WM. Appl Opt 1989;28:1401–8.
[38] Giver LP, Boese RW, Miller JH. JQSRT 1974;14:793–802.
[39] AFGL compilation of atmospheric absorption line parameters. USA National Climatic Centre of NOAA, digital product section, Asheville, NC 28801, USA, reported in Ref. [35].
[40] Caccin B, Cavallini F, Ceppatelli G, Righini A, Sambuco AM. Astron Astrophys 1985;149:357–64.
[41] Gamache BR, Goldman A, Rothman LS. JQSRT 1998;59:495–509.